

## CASE STUDY

## Experimental Evidence for Anomalous Scale Dependent Cascading Process in Turbulent Velocity Statistics

A. Arneodo,<sup>1</sup> S. Manneville,<sup>1</sup> J. F. Muzy,<sup>1</sup> and S. G. Roux<sup>1</sup>*Communicated by Charles K. Chui on March 10, 1998*

We use a wavelet-based deconvolution method to extract some multiplicative cascading process from experimental turbulent velocity signals. We show that at the highest accessible Reynolds numbers, the experimental data do not allow us to discriminate between various phenomenological cascade models recently proposed to account for intermittency and their log-normal approximations. We further report evidence that velocity fluctuations are not scale invariant but possess more complex self-similarity properties that are likely to depend on the Reynolds number. We comment on the possible asymptotic validity of the multifractal description. © 1999

Academic Press

One of the challenging questions in fully developed turbulence is the possible existence of universal scaling behavior as a result of strong nonlinear interactions [1, 2]. In this respect, a very important issue is the scaling properties of velocity structure functions,

$$S_p(l) = \langle \delta v_l^p \rangle \sim l^{\zeta(p)}, \quad (1)$$

where  $\delta v_l(x) = v(x+l) - v(x)$  is a longitudinal velocity increment over a distance  $l$ . The Kolmogorov (K41) theory [3], based on the assumptions of statistical homogeneity and isotropy and of constant rate  $\epsilon$  of energy transfer from large to small scales, predicts the existence of an inertial range  $\eta \ll l \ll L$ , where  $S_p(l) \sim \epsilon^{p/3} l^{p/3}$ . However, there has been increasing numerical and experimental evidence [1, 2, 4–8] that  $\zeta(p)$  deviates nonlinearly from the K41 prediction  $\zeta(p) = p/3$  at large  $p$ . This is generally interpreted as a direct consequence of the intermittency phenomenon displayed by the rate of energy transfer [9, 10]. In the framework of the multifractal description pioneered by Frisch and Parisi [11], the nonlinearity of  $\zeta(p)$  can be seen as the consequence of spatial fluctuations in the local regularity of the velocity field. Over the past 30 years, many theoretical and

<sup>1</sup> Address: Centre de Recherche Paul Pascal, CNRS UPR 8641, Université Bordeaux I, Avenue Schweitzer, 33600 Pessac, France.

phenomenological models have been proposed to account for intermittency. Since the log-normal model early designed by Kolmogorov and Obukhov [12] (KO62), most of the models proposed in the literature are of multiplicative hierarchical nature in order to mimic the energy cascading process (for a review, see Ref. [10]). Unfortunately, all existing models, including the recently proposed log-infinitely divisible cascades [13–16], appeal to adjustable parameters that are difficult to determine by plausible physical arguments and that generally provide enough freedom to account for the experimental data. Therefore, it is not such a surprise that the experimental determination of the  $\zeta(p)$  spectrum fails to provide a selective test to discriminate between various cascade models.

In order to go beyond this multifractal description, Castaing *et al.* [9, 16, 17] have proposed to model the evolution of the shape of the velocity increment pdf from Gaussian at large scales to more intermittent profiles with stretched exponential-like tails at smaller scales [5, 9, 18], by a functional equation that relates two scales  $l' > l$  using a kernel  $G$ :

$$P_l(\delta v) = \int G_{ll'}(\ln r) \frac{1}{r^2} P_r\left(\frac{\delta v}{r}\right) dr. \quad (2)$$

Most of the well-known cascade models can be reformulated within this approach. From Eq. (2), for any decreasing sequence of scales  $(l_1, \dots, l_n)$ , one has  $G_{l_n l_1} = G_{l_n l_{n-1}} \otimes \dots \otimes G_{l_2 l_1}$ , where  $\otimes$  denotes the convolution product. The cascade is said to be continuously self-similar [9, 16] if there exists a positive, monotonous function  $s(l)$ , such that  $G_{ll'}$  depends on  $l$  and  $l'$  only through  $s(l, l') = s(l) - s(l')$ :  $G_{ll'}(x) = G(x, s(l, l'))$ .  $s(l, l')$  actually accounts for the number of cascade steps from scale  $l'$  to scale  $l$ . According to Novikov's definition [13], the cascade is scale-similar if  $s(l, l') = \ln(l'/l)$  ( $s(l) = \ln(L/l)$ ). In their original work, Castaing *et al.* [9] have developed a formalism which is consistent with the KO62 [12] general ideas of log-normality and which predicts an anomalous power-law behavior of the depth of the cascade  $s(l) \sim (l/L)^{-\beta}$ . From the computation of the scaling behavior of the variance of the kernel  $G_{ll'}$ , they have checked [9, 17] that the above-mentioned power law could provide a reasonable explanation of some deviation from scaling observed experimentally on the statistics of velocity fluctuations [8, 19]. The aim of this letter is to process turbulent velocity data for various flow configurations using a method recently proposed to study random cascade processes from wavelet analysis [20].

The wavelet transform (WT) has already proven to be a powerful tool for multifractal analysis of singular distributions including functions [21]. Let us recall that the WT of a function  $f$  is defined as

$$T_\psi[f](x, a) = \frac{1}{a} \int_{-\infty}^{+\infty} f(y) \psi\left(\frac{y-x}{a}\right) dy, \quad (3)$$

where  $x$  is the space position,  $a(>0)$  the scale parameter, and  $\psi$  the analyzing wavelet. Note that for  $\psi(x) = \psi_{(0)}^{(1)}(x) = \delta(x-1) - \delta(x)$ ,  $T_\psi[f](x, a)$  is nothing but the increment  $\delta f_a(x)$  over a distance  $a$ . The WTMM method consists in computing the following partition functions restricted to the WT skeleton defined, at each scale  $a$ , by the WT modulus maxima  $x_i$  [21]:

$$Z(q, a) = a \sum_{x_i} |T_{\psi}[f](x_i, a)|^q \sim a^{\zeta(q)}. \quad (4)$$

$Z(q, a)$  can be seen as a generalization of the structure functions defined in Eq. (1) in the sense that it allows an estimation of  $\zeta(q)$  for  $q < 0$  (for details see Ref. [21]). Throughout this study, we will use the set of compactly supported analyzing wavelets defined in Ref. [20] and more specifically  $\psi_{(m)}^{(1)}$  that are smooth versions of  $\psi_{(0)}^{(1)} = \delta(x - 1) - \delta(x)$  obtained after  $m$  successive convolutions with the box function  $\chi$ . We have checked that all the results reported below are consistent when changing both the regularity and the order of  $\psi$ . The arborescent space-scale structure of the WT skeleton is likely to contain all the information about some underlying multiplicative process [21]. Along the line of Castaing *et al.* ansatz [9, 16], the pdf  $P_a(T)$  of the WTMM coefficients at scale  $a$  can be expressed as a weighted sum of dilated pdfs at a different scale  $a' > a$ , very much like Eq. (2) for the velocity increments. As demonstrated in Ref. [20], if one notes  $M(p, a) = \int e^{ip \ln(|T|)} P_a(T) dT$ , the characteristic function associated to the logarithm of the WTMM coefficients at scale  $a$ , then the Fourier transform  $\hat{G}$  of the kernel  $G$  can be computed as  $\hat{G}_{aa'}(p) = M(p, a)/M(p, a')$ , provided  $M(p, a')$  do not vanish. Note that from the convolution property of  $G$  and the additivity of the function  $s$ , the cascade is continuously self-similar if  $\hat{G}_{aa'}$  can be expressed as

$$\hat{G}_{aa'}(p) = \hat{G}(p)^{s(a, a')}. \quad (5)$$

Let us now proceed to the analysis of experimental turbulent velocity signals. The data were recorded by Gagne *et al.* [5, 9]. We use the Taylor hypothesis to identify temporal and spatial variations of the longitudinal velocity component. We focus on two experiments corresponding to a wind tunnel ( $R_\lambda = 3050$ ) and a laboratory jet ( $R_\lambda = 835$ ) flows. Our samples represent a statistics of  $1.5 \times 10^7$  points ( $1000L$ ) with resolution  $\Delta x \approx 1.2\eta$  for the wind tunnel data and of about  $2.1 \times 10^7$  points ( $2500L$ ) with resolution  $\Delta x \approx 2\eta$  for the jet, where  $\eta$  and  $L$  are the corresponding dissipative and integral scales. In Figs. 1a and 2a, we report the results of both WTMM [21] and structure function analysis. From Fig. 1a, one may fairly say that  $Z(q, a)$  follows a power law in the inertial range. However, the scaling behavior is rather approximative for  $R_\lambda = 835$  since a curvature is clearly visible on the log–log plots. Even weaker, such a curvature is still there at higher Reynolds number  $R_\lambda = 3050$ . In Fig. 2a are reported the estimate of the  $\zeta(q)$  scaling exponents from linear regression fit of the data over the inertial range of scales indicated in Fig. 1a. Two main observations have to be stressed. For the wind tunnel signal, the  $\zeta(q)$  spectrum computed with  $\psi_{(3)}^{(1)}$  lies significantly below the one computed with  $\psi_{(0)}^{(1)}$  for  $q \geq 3$ . This discrepancy strongly questions the possible existence of a scale invariant self-similar cascade, since for these processes  $\zeta(q)$  is expected to be independent of the shape of the analyzing wavelet [20, 21]. For the jet signal, the  $\zeta(q)$  spectrum computed with the WTMM method strongly deviates from the one of the wind tunnel signal, as soon as  $q \geq 2$ . This difference questions the possible universality [8] of the  $\zeta(q)$  exponents with respect to the Reynolds number. However, as suggested by the notion of extended self-similarity (ESS) [19], if one plots  $\ln[Z(q, a)/Z(0, a)]$  vs  $\ln[Z(3, a)/Z(0, a)]$ , one undoubtedly improves scaling. As shown in Fig. 2a, the so-obtained  $\zeta(q)$  spectra

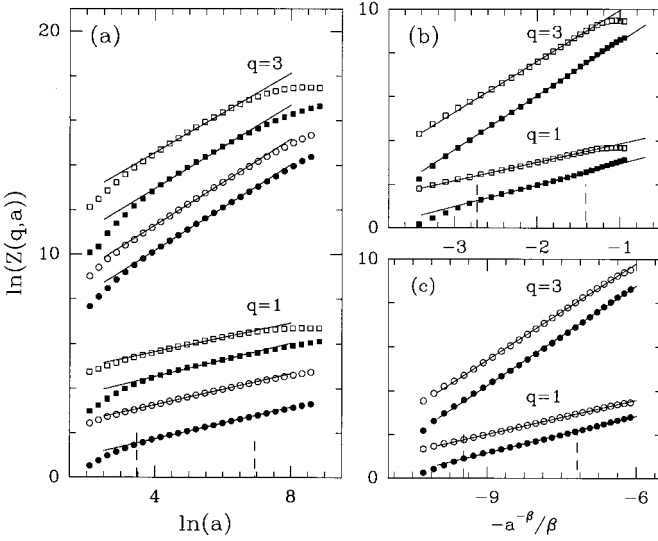


**FIG. 1.** WTMM computation of  $Z(q, a)$  for  $q = 1$  and  $3$ ;  $a$  is expressed in  $\eta$  units. (a)  $\ln Z(q, a)$  vs  $\ln a$  for the jet ( $\square, \blacksquare$ ) and wind tunnel ( $\circ, \bullet$ ) velocity signals. (b)  $\ln Z(q, a)$  vs  $-a^{-\beta}/\beta$  for the jet signal with  $\beta = 0.19$ . (c) Same as in (b) but for the wind tunnel signal with  $\beta = 0.08$ . The analyzing wavelet is  $\psi_{(3)}^{(1)}$  ( $\blacksquare, \bullet$ ). The symbols ( $\square, \circ$ ) correspond to classical structure function calculations.

no longer depend upon the analyzing wavelet and are almost undistinguishable for both experiments. Note that, over a range of values of  $q$  that extends from  $-3$  to  $+6$ , for which statistical convergence is achieved, the predictions of both the log-normal [12, 20] and log-Poisson [15, 20] models provide very good fits of the experimental  $\zeta(q)$  spectrum.

In Fig. 3 are represented the modulus and the phase of the kernel  $\hat{G}_{aa}(p)$  that we

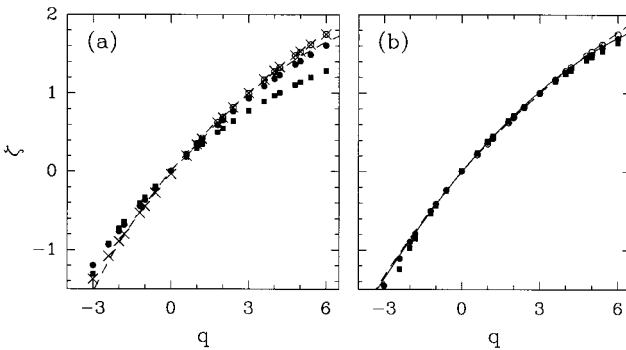


**FIG. 2.** (a) WTMM vs structure function computation of the  $\zeta(q)$  spectrum (from Fig. 1a). Jet velocity signal: ( $\blacksquare$ ) WTMM with  $\psi_{(3)}^{(1)}$ , ( $- -$ ) WTMM with ESS. Wind tunnel velocity signal: ( $\circ$ ) structure functions, ( $\bullet$ ) WTMM with  $\psi_{(3)}^{(1)}$ , ( $\times$ ) WTMM with ESS. (b)  $\zeta(q)$  spectrum obtained when assuming the validity of Eq. (6) (from Figs. 1b and 1c): Jet ( $\blacksquare$ ) and wind tunnel ( $\bullet$ ) velocity signals. For comparison the  $\zeta(q)$  spectrum of the wind tunnel signal obtained with the structure function method and ESS is shown ( $\circ$ ). The solid line corresponds to a fit of the data with the log-normal model [12]:  $\zeta(q) = mq - \sigma^2 q^2/2$  with  $m = 0.40$  and  $\sigma^2 = 0.038$ . The dashed line corresponds to the She and Leveque log-Poisson model [14]:  $\zeta(q) = q/9 + 2(1 - (\frac{2}{3})^{q/3})$ .

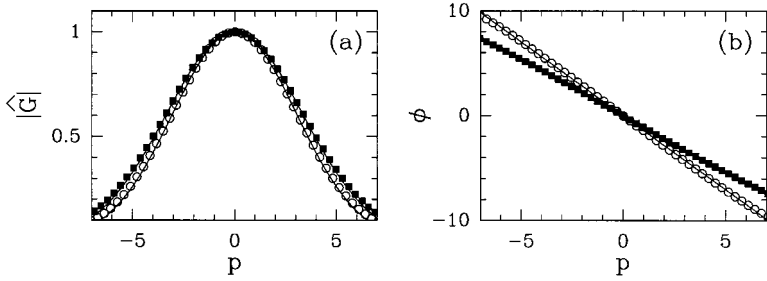


**FIG. 3.** Numerical computation of  $\hat{G}_{aa'}(p)$  for the jet (■) and wind tunnel (○) signals. The analyzing wavelet is  $\psi_{(3)}^{(1)}$ ,  $a = 2^5$  and  $a' = 2^{11}$ . (a)  $|\hat{G}_{aa'}|$  vs  $p$ ; (b)  $\phi_{aa'} = \arctan(\text{Im} \hat{G}_{aa'}/\text{Re} \hat{G}_{aa'})$  vs  $p$ . The solid lines represent fits of the data with a log-normal kernel:  $|\hat{G}_{aa'}| = \exp(-p^2\sigma^2(a, a')/2)$ ,  $\phi_{aa'} = -m(a, a')p$ .

numerically estimate in the inertial range. As long as  $50\eta \leq a < a' \leq L$ , this kernel is found to be very well fitted, for  $-6 \leq p \leq 6$ , by the Fourier transform of a log-normal kernel:  $\hat{G}_{aa'}(p) = \exp(-ipm(a, a') - p^2\sigma^2(a, a')/2)$ . Actually we have checked that the cumulants of  $G$  of order higher than 2 are negligible for both flows. Thus, with the available statistics, one cannot distinguish, for these Reynolds numbers, the various log-infinitely divisible cascade models [13–16] including the log-Poisson model [14, 15] from their log-normal approximations. In order to test scale similarity or more generally the pertinence of Eq. (5), we have plotted in Figs. 4a and 4c,  $m(a, a') = \partial \text{Im}(\hat{G}_{aa'})/\partial p|_{p=0}$  and  $\sigma^2(a, a') = -\partial^2(\ln|\hat{G}_{aa'}|)/\partial p^2|_{p=0}$ , respectively, as functions of  $s(a, a') = \ln(a'/a)$  for different couples of scales  $(a, a')$  in the inertial range. It is striking for the jet data, but also noticeable for the wind tunnel data, that the curves obtained when fixing the largest scale  $a'$  and varying the smallest one  $a$  have a clear bending and do not merge

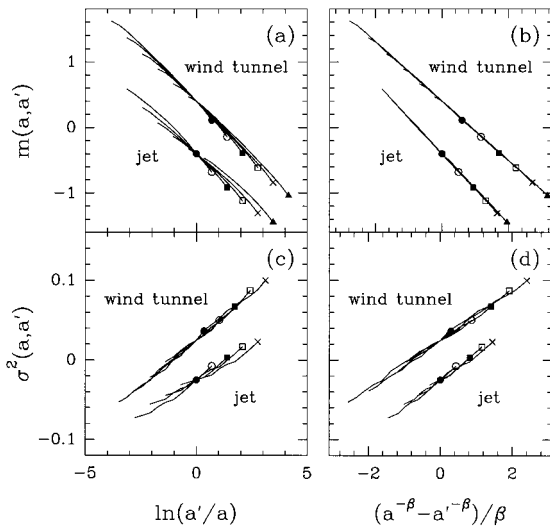


**FIG. 4.**  $m(a, a')$  and  $\sigma^2(a, a')$  as computed for the jet and wind tunnel velocity signals for  $a' = 2^6$  (●),  $2^7$  (○),  $2^8$  (■),  $2^9$  (□), and  $2^{10}$  (×). (a)  $m(a, a')$  vs  $\ln(a'/a)$ ; (b)  $m(a, a')$  vs  $(a^{-\beta} - a'^{-\beta})/\beta$ ; (c)  $\sigma^2(a, a')$  vs  $\ln(a'/a)$ ; (d)  $\sigma^2(a, a')$  vs  $(a^{-\beta} - a'^{-\beta})/\beta$ . In (b) and (d),  $\beta = 0.19$  (jet) and  $\beta = 0.08$  (wind tunnel).

on the same straight line as expected for scale-similar cascade processes. In Figs. 4b and 4d, the same data are plotted versus  $s(a, a') = (a^{-\beta} - a'^{-\beta})/\beta$  with  $\beta = 0.08$  for the wind tunnel flow and  $\beta = 0.19$  for the jet flow. In these cases, the data for the mean  $m(a, a')$  and the variance  $\sigma^2(a, a')$  fall, respectively, on one unique line. The velocity fields we have analyzed therefore are not scale-similar but rather are characterized by some anomalous behavior of the number of cascade steps between scale  $a'$  and scale  $a$ :  $s(a, a') = (a^{-\beta} - a'^{-\beta})/\beta$ . This behavior differs from the pure power law prompted by Castaing *et al.* [9, 17]. As far as the multifractal WTMM analysis is concerned, this behavior leads to the following function form for  $Z(q, a)$  [20],

$$Z(q, a) = C_1 e^{-C_2 a^{-\beta} \zeta(q)}, \quad (6)$$

instead of the classical power law (Eq. (4)). Let us emphasize that this form has been predicted by Dubrulle [22] by simple symmetry considerations. If one plots  $\ln Z(q, a)$  versus  $-a^{-\beta}/\beta$  (instead of  $\ln a$ ), one can see in Figs. 1b and 1c that for both the jet and wind tunnel data, the systematic curvature observed in Fig. 1a disappears. The estimate of the corresponding  $\zeta(q)$  exponents obtained from linear regression fits are reported in Fig. 2b; the data remarkably fall on a quadratic curve as predicted for log-normal cascade processes. These exponents no longer depend on the specific shape of the analyzing wavelet  $\psi$  and are indistinguishable from those previously obtained in Fig. 2a when using ESS. This is not surprising since Eq. (6) is compatible with ESS. Moreover, one does not see any significant difference between the  $\zeta(q)$  exponents extracted from the jet and the wind tunnel turbulent signals. This observation suggests the possible universality of the  $\zeta(q)$  spectrum [8] for high Reynolds number isotropic turbulence. Let us point out that a real test of log-normality would be to see the decrease of  $\zeta(q)$  at large  $q (> 0)$ . According to the fit reported in Fig. 2b, the  $\zeta(q)$  spectrum should decrease for  $q \geq 11$ , in qualitative agreement with previous discussions [9, 18]: reaching an acceptable statistical convergence for  $q \approx 12$  would require velocity records one hundred times larger than those processed in this work.

The exponent  $\beta$  somehow quantifies the departure from scale similarity since in the limit  $\beta \rightarrow 0$ ,  $s(a, a') = (a^{-\beta} - a'^{-\beta})/\beta$  reduces to  $\ln(a'/a)$ . In Fig. 5 are reported the estimate of  $\beta$  as a function of the Reynolds number (the three additional points at  $R_\lambda = 2000, 600$ , and  $280$  correspond, respectively, to wind tunnel, jet, and grid turbulence). In Fig. 5a,  $\beta$  is plotted versus  $1/\ln(R_\lambda)$  in order to check experimentally the validity of some theoretical arguments developed in Refs. [9, 22] which predict a logarithmic decay of  $\beta$  when increasing  $R_\lambda$ . Indeed the data are very well fitted by  $\beta \sim 1/\ln(R_\lambda) - 1/\ln(R_\lambda^*)$ , where  $R_\lambda^* \approx 12000$ , which suggests that scale similarity is likely to be attained at finite Reynolds numbers. However, as shown in Fig. 5b, the data are equally very well fitted by a power-law decay  $\beta \approx 1/R_\lambda^{0.556}$  with an exponent which is found close to  $\frac{1}{2}$ . This second possibility brings the clue that scale similarity might well be valid only in the limit of infinite Reynolds number. Whatever the relevant  $\beta$  behavior, our findings for the kernel  $G_{aa'}$  strongly indicate that at very high Reynolds numbers, intermittency can be understood in terms of a continuous self-similar multiplicative process that converges toward a scale-similar log-normal cascade, discarding the possible asymptotic validity of K41 theory [3]. As emphasized by Frisch [2], such statistics for the velocity fluctuations imply

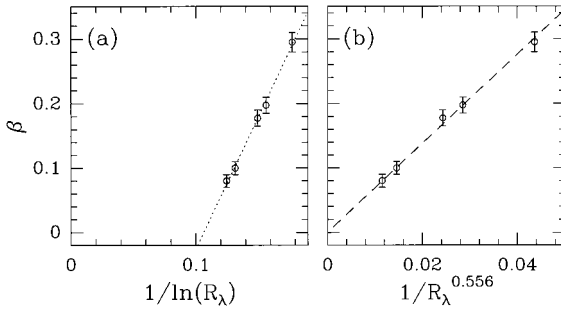


**FIG. 5.**  $\beta$  as a function of the Reynolds number. (a)  $\beta$  vs  $1/\ln(R_\lambda)$ ; the dotted line corresponds to a fit of the data with  $\beta = B(1/\ln(R_\lambda) - 1/\ln(R_\lambda^*))$  and  $R_\lambda^* = 12000$ . (b)  $\beta$  vs  $1/R_\lambda^{0.556}$ ; the dashed line corresponds to a linear regression fit of the data. Error bars account for variation of  $\beta$  according to the definition of the inertial range.

that the Mach number of the flow increases indefinitely, which invalidates the assumption of incompressible flows. This observation does not, however, violate the basic laws of hydrodynamics since it is conceivable that, at extremely high Reynolds numbers, supersonic velocities might appear.

### ACKNOWLEDGMENTS

We are very grateful to Y. Gagne and Y. Malecot for the permission to use their experimental data. This work was supported by "Direction des Recherches, Etudes et Techniques" under Contract DRET 95/11.

### REFERENCES

1. A. S. Monin and A. M. Yaglom, "Statistical Fluid Mechanics," Vol. 2, MIT Press, Cambridge, MA, 1975.
2. U. Frisch, "Turbulence," Cambridge Univ. Press, Cambridge, UK, 1995.
3. A. N. Kolmogorov, *C. R. Acad. Sci. USSR* **30** (1941), 301.
4. F. Anselmet, Y. Gagne, E. J. Hopfinger, and R. A. Antonia, *J. Fluid Mech.* **140** (1984), 63.
5. Y. Gagne, Thesis, University of Grenoble, 1987.
6. A. Vincent and M. Meneguzzi, *J. Fluid Mech.* **225** (1995), 1.
7. P. Tabeling and O. Cardoso, Eds., "Turbulence: A Tentative Dictionary," Plenum, New York, 1995.
8. A. Arneodo *et al.*, *Europhys. Lett.* **34** (1996), 411.
9. B. Castaing, Y. Gagne, and E. J. Hopfinger, *Physica D* **46** (1990), 177.
10. C. Meneveau and K. R. Sreenivasan, *J. Fluid Mech.* **224** (1991), 429.
11. U. Frisch and G. Parisi, in "Turbulence and Predictability in Geophysical Fluid Dynamics and Climate Dynamics" (M. Ghil, R. Benzi, and G. Parisi, Eds.), p. 84, North-Holland, Amsterdam, 1985.
12. A. N. Kolmogorov, *J. Fluid Mech.* **13** (1962), 82; A. M. Obukhov, *J. Fluid Mech.* **13** (1962), 77.
13. E. A. Novikov, *Phys. Fluids A* **2** (1990), 814; *Phys. Rev. E* **50** (1995), 3303.
14. Z. S. She and E. Leveque, *Phys. Rev. Lett.* **72** (1994), 336.
15. B. Dubrulle, *Phys. Rev. Lett.* **73** (1994), 959; Z. S. She and E. C. Waymire, *Phys. Rev. Lett.* **74** (1995), 262.
16. B. Castaing and B. Dubrulle, *J. Physique II* **5** (1995), 895.
17. B. Castaing, Y. Gagne, and M. Marchand, *Physica D* **68** (1993), 387; A. Naert, L. Puech, B. Chabaud, J.

- Peinke, B. Castaing, and B. Hébral, *J. Physique II* **4** (1994), 215; B. Chabaud, A. Naert, J. Peinke, F. Chillà, B. Castaing, and B. Hébral, *Phys. Rev. Lett.* **73** (1994), 3227.
18. F. Belin, P. Tabeling, and H. Willaime, *Physica D* **93** (1996), 52.
19. R. Benzi, S. Ciliberto, C. Baudet, and G. Ruiz-Chavarria, *Physica D* **80** (1995), 385.
20. A. Arneodo, J. F. Muzy, and S. G. Roux, *J. Physique II* **7** (1997), 363; S. G. Roux, Ph.D. thesis, University of Aix-Marseille II, 1996.
21. (a) J. F. Muzy, E. Bacry, and A. Arneodo, *Phys. Rev. Lett.* **67** (1991), 3515; *Phys. Rev. E* **47** (1993), 875; *Internat. J. Bifur. Chaos* **4** (1994), 245; (b) A. Arneodo, E. Bacry, and J. F. Muzy, *Physica A* **213** (1995), 232.
22. B. Dubrulle, *J. Physique II* **6** (1996), 1825.